Catalysis Today 172 (2011) 13–20

Contents lists available at ScienceDirect

Catalysis Today

journal homepage: www.elsevier.com/locate/cattod

Pt and Pd nanoparticles supported on structured materials as catalysts for the selective reductive amination of carbonyl compounds

Marcelo E. Domine[a,*], M. Consuelo Hernández-Soto[a], María T. Navarro[a], Yolanda Pérez[b]

[a] Instituto de Tecnología Química (UPV-CSIC), Universidad Politécnica de Valencia, Consejo Superior de Investigaciones Científicas, Avenida de los Naranjos s/n, 46022 Valencia, Spain
[b] Universidad Rey Juan Carlos, Tulipán s/n, 28933 Móstoles, Madrid, Spain

ARTICLE INFO

Article history:
Received 1 March 2011
Received in revised form 10 May 2011
Accepted 11 May 2011
Available online 16 June 2011

Keywords:
Pt nano-particles
Pd nano-particles
Metal catalysts
Bi-functional catalysts
Reductive amination

ABSTRACT

Metal catalysts based on Pt and Pd nano-particles supported on structured microporous Beta zeolites and mesoporous MCM-41 materials, as well as specially designed γ-Al_2O_3 samples, were synthesized following a simple and economic procedure. Physico-chemical characterization of metal-composites (by XRD, IR spectroscopy, TEM, N_2 adsorption, ICP, among others) indicated that both Pt and Pd nano-particles were adequately supported and homogeneously dispersed on supports. These metal/solid acid composites were applied as efficient catalysts under mild reaction conditions in the selective reductive amination of ketones, a useful industrial reaction for the synthesis of substituted amines and N-heterocycles. Results obtained showed that Pt/Al-Beta catalyst possesses the best catalytic activity (TON = 1610, with amine selectivities >95%) superior to that observed with commercial Pt/C and Pt/Al_2O_3 (TON $\approx$ 1000). Enhancements in Pt/Al-Beta samples were achieved by optimizing the Pt loading, and mainly the Si/Al molar ratio in solids. On the contrary, inferior catalytic activities were encountered with the Pt/Si-MCM-41 and Pt/Al-MCM-41 materials. The Pd incorporation on MCM-41 materials produced more active catalysts than the commercial Pd/C and Pd/Al_2O_3 samples. Finally, the study of Pt/ and Pd/γ-Al_2O_3 materials demonstrated that the treatments of support prior to the metal impregnation and the posterior calcinations processes were essentials to obtain efficient catalysts.

1. Introduction

Substituted amines [1] and several both aromatic and aliphatic N-heterocycles, such as pirazines and piperazines, respectively [2–5], are useful intermediates for the preparation of pharmaceutical and agro-chemical products. These nitrogen-containing compounds are commonly synthesized by reduction of the corresponding (di)ketopiperazines or by various cyclization reactions, for example, by dialkylation of amines with bis(2-chloroethyl)amine, or by intramolecular reductive coupling of diamines [6,7]. However, some attempts have been made in the synthesis of these substituted amines and N-heterocycles by using multi-step reactions involving consecutive addition, cyclization, and reduction of alcohols, aldehydes or ketones with amines in the presence of metal supported solid catalysts [8–10]. It is fairly accepted that the most important steps taking place in the overall process can be recognized as the main pathways included in reductive amination-type reactions, such as (i) addition, (ii) dehydration towards the imine or enamine intermediate (depending on the primary or secondary starting amine used, respectively), and (iii) imine or enamine reduction to produce the substituted amine (Scheme 1) [11]. When carbonyl compounds are used as starting reactants, the hydrogenation of enamine or imine intermediates is the slowest step of the process, this being the reason for working under H_2 addition at moderate to high temperature during reaction [12].

In the past years, the most commonly used catalysts for the reductive aminations of aldehydes or ketones with amines were mixed metal oxides and metal-zeolites (metal = Cu, Zn, Ni, and Co) [2–5,11], while some Ru(II) and Ir(I) homogeneous complexes [13–15], as well as Ni-Raney [16], were reported as catalysts for the reductive aminations performed at high H_2 pressures and temperatures with the less reactive alcohols. In the later case, the proposed reaction mechanism includes a first step of oxidative dehydrogenation of the alcohol to the corresponding carbonyl compound [8–11], this being the determinating reaction step. This fact explains the low reactivity and the elevated temperatures needed to obtain the desired substituted amines starting from the alcohols. If the objective is to carry out the reductive amination under mild reaction conditions, metal active sites capable to perform the imine or enamine selective reduction by working at low both temperatures and H_2 pressures are needed. In this sense, we have recently demonstrated [10] that controlled size Pt and Pd nanoparticles supported on solid metal oxides (with adequate acid–base properties, high

* Corresponding author. Tel.: +34 963879696; fax: +34 963877809.
E-mail address: mdomine@itq.upv.es (M.E. Domine).

0920-5861/$ – see front matter © 2011 Elsevier B.V. All rights reserved.
doi:10.1016/j.cattod.2011.05.013

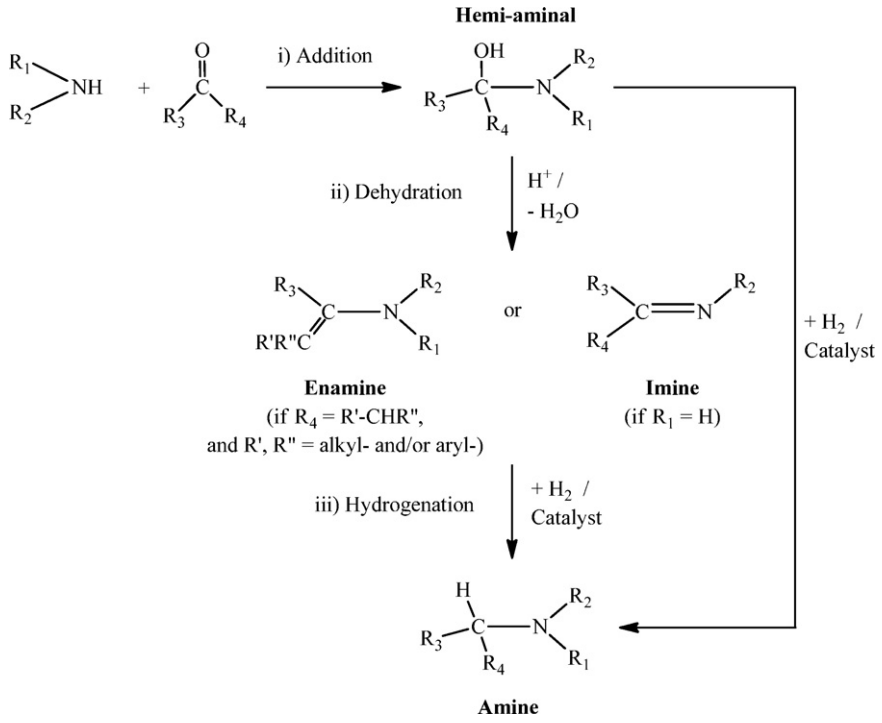

Scheme 1. Reaction steps and intermediates proposed in the reductive amination of carbonyl compounds.

surface area, and particle size) can dissociate the H_2 molecule at low temperature and, importantly, when H_2 is present on the catalytic surface in low concentrations. Moreover, if solid supports possessing well controlled acid/base properties and porosity are selected, it could be possible to design effective and selective multi-functional catalysts for the reductive amination process.

In this work, we have prepared several catalytic materials based on Pt and Pd nanoparticles supported on Beta zeolites, MCM-41 mesoporous materials, and also regular alumina. Their synthesis and characterization will be described, whereas their catalytic application in the reductive amination of ketones under mild reaction conditions in the absence of solvent will also be depicted. The influences of the type of metal, and both acid–base and textural properties of supports on the catalytic activities will be studied, these activities being compared with commercial catalysts and other Me-supported materials commonly used in this process.

2. Experimental procedure

2.1. Materials

Cyclohexanone (99.8%), 2-hexanone (98%), 2-octanone (98%), piperidine (99%), and *n*-nonane (99%) were purchased from Sigma–Aldrich and used as received. Acetone, acetonitrile, 2-propanol (Scharlau, analytical grade, 99.5%), and water (Milli-Q quality, Millipore) were used as solvents, whereas hydrogen 5.0 (Abelló Linde S.A., 99.999%) was used as reduction agent. For catalysts synthesis the following reactants were used: tetraethyl-ammonium hydroxide (TEAOH, Aldrich, 35 wt% in water), tetraethyl-orthosilicate (TEOS, Merck, >98%), cetyl-trimethyl-ammonium bromide (C16TMABr, Aldrich), tetramethyl-ammonium hydroxide (TMAOH, Aldrich, 25 wt% in water), HF (Aldrich, 48 wt% in water), silica gel (Aerosil 200, DEGUSSA), pseudobohemite (60 wt% de Al_2O_3), γ-Al_2O_3 (Aldrich), and aluminium *iso*-propoxide (Aldrich, 99%). $Pd(NH_3)_4Cl_2{\cdot}H_2O$ (Aldrich, 99.99+%), and $H_2PtCl_6{\cdot}6H_2O$ (Aldrich, ≥37.5% Pt basis) were used as metal sources.

For comparative purposes the following commercial catalysts supplied by Aldrich were also used: 5 wt% Pt/C, 5 wt% Pd/C, 5 wt% Pt/Al_2O_3, and 5 wt% Pd/Al_2O_3.

2.2. Catalysts preparation

2.2.1. Synthesis of Beta zeolites microporous materials

Al-Beta and Si-Beta (pure siliceous) hydrophobic zeolites were synthesized in fluoride media following the methodology described in Ref. [17], through hydrothermal synthesis at 140 °C in Teflon-lined stainless-steel autoclaves with rotation (60 rpm). The Al-Beta (Si/Al = 50) was synthesized by mixing 20.0 g of TEOS, 21.8 g of TEAOH (35 wt% in water), 0.39 g of aluminium *iso*-propoxide, and 5.0 g of water. The mixture was kept under stirring until the complete evaporation of the ethanol formed upon hydrolysis of TEOS. Finally, HF (48 wt% in water) and, optionally, dealuminated zeolite beta seeds were added, thus obtaining the following gel composition (in mol): SiO_2:0.01 Al_2O_3:0.54 TEAOH:7.5 H_2O:0.54 HF. After the required crystallization time, the autoclaves were cooled and the solids were filtered and extensively washed with distilled water. The Si/Al ratio was 50 as determined from chemical analysis (ICP). Finally, the solids were dried at 100 °C and calcined at 580 °C during 3 h, and the resultant materials were analyzed by XRD showing high crystallinities (>93%), and also by other available techniques (crystal size ≈ 0.3 μm, micropore volume = 0.19 cm^3/g).

The Si-Beta material was prepared by mixing 30 g of TEOS and 33 g of TEAOH (35 wt% in water), and dealuminated zeolite beta seeds were also added (0.36 g of dealuminated zeolite beta in 1.5 g of water), thus starting from the following gel composition (in mol): SiO_2:0.27 TEA_2O:0.54 HF:7.5 H_2O. This Si-Beta zeolite (crystal size ≈ 1.0 μm, micropore volume = 0.20 cm^3/g) showed a high crystallinity (>93%), the later was maintained after calcination at 580 °C.

2.2.2. Synthesis of MCM-41 mesoporous materials

The mesoporous materials Al-MCM-41 (Si/Al = 50) and Si-MCM-41 were prepared according with the procedure described in Ref. [18]. Thus, 9.11 g of C16TMABr dissolved in 61.11 g of water (Milli-

Q) were mixed with 15.77 g of TMAOH (25 wt% in water). The mixture was homogeneized and 0.27 g of $Al(OH)_3$ (60 wt% Al_2O_3) were added. The mixture was stirred during 5 min and then 10 g of silica gel (Aerosil 200) were added, the stirring being maintained during 1 h. The resulting gel possessed the following molar composition: SiO_2:0.1 Al_2O_3:0.16 C16TMABr:0.26 TMAOH:24.3 H_2O. The gel was placed in a Teflon-lined stainless-steel autoclave and heated at 135 °C under static conditions for 24 h. The resulting solid was filtered, washed with water, and dried at 60 °C for 24 h. The occluded organic was removed by calcination treatment at 540 °C during 6 h. In the case of Si-MCM-41, the addition of the metal source was eliminated. The solid obtained presents a surface area of ≈1000 m^2/g with 3.5 nm pore diameter (35 Å), and XRD pattern of MCM-41 structure (spectra not shown), while the Si/Al ratio was determined by chemical analysis (ICP).

2.2.3. Synthesis of high surface γ-Al_2O_3

The amorphous γ-Al_2O_3 (surface area > 300 m^2/g) was synthesized following the procedure detailed in the Ref. [19]. The obtained gel was treated by calcination in air at two different temperatures 500 °C and 800 °C, thus obtaining the γ-Al_2O_3[C5] and γ-Al_2O_3[C8] samples, respectively. Additionally, alumina samples were also treated by lyophilisation [L] followed by calcination in air at 500 °C to obtain the corresponding γ-Al_2O_3[LC5] material. All alumina samples were characterized by XRD, TGA–DTA, and N_2 adsorption isotherms, among others.

2.2.4. Pd and Pt incorporation on different metal oxides as supports

In general, metal incorporation on different previously calcined metal oxides was performed by the incipient wetness impregnation method using aqueous solutions of $Pd(NH_3)_4Cl_2{\cdot}H_2O$ and $H_2PtCl_6{\cdot}6H_2O$ as Pd and Pt sources, respectively. The solid samples were dried in oven at 100 °C overnight, and then calcined at the corresponding temperature above-mentioned depending on the type of support used. Thus the obtained catalytic materials were activated under H_2 flow (100 ml/min) at 350 °C during 3 h before use. Metal loadings on solids were determined by chemical analyses (ICP), whereas metal nanoparticles size and distribution on different supports were measured by TEM, and corroborated by CO chemical-adsorption measurements.

2.3. Catalysts characterization

Phase purity of the catalysts was determined by X-ray diffraction (XRD) in a Philips X'Pert MPD diffractometer equipped with a PW3050 goniometer (CuKα radiation, graphite monochromator), provided with a variable divergence slit and working in the fixed irradiated area mode. Diffuse reflectance UV–vis (DRUV) spectra of samples were recorded in a Cary 5 Varian spectrometer equipped with a "Praying Mantis" cell from Harrick. Infrared spectra were obtained in a Nicolet 710 FTIR spectrometer using self-supported wafers of 10 mg/cm^2 outgassed overnight at 653 K and 10^{-3} Pa.

Thermogravimetric and differential thermal analyses (TGA–DTA) were performed in a Netzsch STA 409 EP thermal analyzer with about 20 mg of sample and a heating rate of 10 °C/min in air flow (6 l/h). Surface area, pore volume, and pore size distribution of the solid samples (200 mg) were calculated by the BET method by carrying out liquid nitrogen and argon adsorption experiments at 77 and 85 K, respectively, in a micromeritics flowsorb apparatus. Pd dispersion in catalysts was estimated from CO adsorption using the double isotherm method in Quantachrome Autosorb-1C equipment. Samples were reduced under H_2 flow at 350 °C for 3 h, and degassed at 1333×10^{-3} Pa for 2 h at the same temperature. Then, the temperature was lowered at 35 °C, and pure CO was admitted for the first adsorption isotherm measurement. After evacuation at 35 °C, the second isotherm was measured. The amount of chemisorbed CO was then obtained by subtracting the two isotherms at the studied pressure range ($0.5–11 \times 10^4$ Pa). The dispersion of Pd was calculated from the amount of irreversibly adsorbed CO assuming a stoichiometry of Pd/CO = 1 was used by other authors [20,21].

Chemical composition was determined by using an inductively coupled plasma emission spectrophotometer Varian 715-ES and elemental analyses in a Fisons EA1108CHN-S. Scanning electron microscopy in a JEOL 6300 microscope was used in order to know the size and morphology of the crystals. Samples for transmission electron microscopy (TEM) were ultrasonically dispersed in ethanol and transferred to carbon coated copper grids. TEM micrographs were collected in a Philips CM-10 microscope operating at 100 kV. Average particle size values were obtained by measuring the diameters of about 100 particles in a representative region.

2.4. Catalytic experiments

Catalytic experiments were performed in a 2.5 ml glass microreactor equipped with a magnetic bar, and sensors for both temperature and pressure control. The reactor had also connections to allow gas supply, and also an outlet for samples to be taken at different time intervals. Typically, equimolecular amounts of piperidine (6 mmol) and the selected ketone (6 mmol) were placed into the reactor followed by catalyst addition (30–50 mg of solid). The reactor was hermetically sealed, pressurised with hydrogen at 5 bars, and heated at 100 °C under continuous stirring. Small liquid aliquots (≈100 μl) were taken, filtered off and diluted in 0.5 g of an *iso*-propanol solution containing 2 wt% *n*-nonane as standard. The liquid samples were analyzed by a 3900-Varian GC equipped with both a FID detector and a capillary column (HP-5, 30 m length). Products identification was done by GC–MS (Agilent 6890N GC System coupled with an Agilent 5973N mass detector) by comparison with commercially available standard, and also by liquid ^1H and ^{13}C NMR spectroscopy.

Amine (and also ketone) conversion and products selectivity (based on GC obtained data) are defined as: (initial moles of reactant – final moles of reactant)/initial moles of reactant × 100, and moles of product *i*/moles of total products × 100, respectively. Turnovers number (TON) here reported is defined as: moles of products/moles of metal on solid.

3. Results and discussion

3.1. Characterization of prepared catalysts

The main physical and textural properties of Pd and Pt nanoparticles supported on regular alumina, Beta zeolite, and MCM-41 mesoporous material are detailed in Tables 1–3, respectively.

In general, lyophilised γ-Al_2O_3 presented higher surface area (420–440 m^2/g) than calcined samples (≈300 and ≈400 m^2/g for 800 and 500 °C calcination temperatures, respectively). Simple pH measurements of these samples revealed that lyophilised sample (pH ≈ 4.3) presented lower pH values than calcined samples (pH around 6.1–6.2). Both Pd (≈1.5%) and Pt (≈2.0%) were homogeneously incorporated onto γ-Al_2O_3 as support, this resulting in metal particle average size of 4–5 nm in all the cases (Table 1). All Pt/Al_2O_3 supported materials showed metal particle diameters around 4–5 nm with a narrow distribution and homogeneously dispersed on alumina surface (TEM images not shown). X-ray diffraction patterns of reduced samples (data not shown) showed the characteristic reflections peaks of Pt (at 2θ = 39.9°, 46.7°, 67.8°, 81.8°, and 86.0°), which evidenced the presence of Pt^0 metallic species on solids. At the same time, XRD diffractograms revealed

Table 1
Physical and textural properties of Pt and Pd supported on γ-Al_2O_3 materials.

Sample [treatment][a]	Metal content (wt%)[b]	Metal particle diam. (nm)[c]	B.E.T. surface area (m^2/g)
Pt/Al_2O_3 [C5]	2.0	4–5	220
Pt/Al_2O_3 [C8]	1.9	4–5	335
Pt/Al_2O_3 [LC5]	1.5	4–5	406
Pd/Al_2O_3 [LC5]	1.4	5	285
γ-Al_2O_3	–	–	420

[a] Treatments: [C5] = calcination at 500 °C, [C8] = calcination at 800 °C, [LC5] = lyophilisation + calcination at 500 °C.
[b] Metal content determined by ICP.
[c] Average metal particle diameter calculated from TEM measurements.

Table 2
Physical and textural properties of Pt and Pd supported on Beta zeolites.

Sample (Si/Al molar ratio)	Metal content (wt%)[a]	Metal particle diameter (nm)[b]	B.E.T. surface area (m^2/g)
Pt/Si-Beta	0.8	2–3	389
Pt/Al-Beta (50)	0.9	4–5	372
Pd/Si-Beta	0.8	10–12	–
Pd/Al-Beta (50)	1.2	8–10	–
Si-Beta	–	–	450
Al-Beta (50)	–	–	484

[a] Metal content determined by ICP.
[b] Average metal particle diameter calculated from TEM measurements.

Table 3
Physical and textural properties of Pt and Pd supported on MCM-41 materials.

Sample (Si/Al molar ratio)	Metal content (wt%)[a]	Metal particle diameter (nm)[b]	B.E.T. surface area (m^2/g)	Pore volume (cm^3/g)
Pt/Si-MCM-41	3.9	2	890	0.58
Pt/Al-MCM-41 (50)	4.1	2–3	820	0.70
Pt/Si-MCM-41	1.9	2–3	857	0.67
Pt/Al-MCM-41 (50)	1.8	3–4	833	0.64
Pd/Si-MCM-41	1.4	11–13	819	0.43
Pd/Al-MCM-41 (50)	1.4	7–9	825	0.66
Si-MCM-41	–	–	1053	0.77
Al-MCM-41 (50)	–	–	975	0.78

[a] Metal content determined by ICP.
[b] Average metal particle diameter calculated from TEM measurements.

that the γ-Al_2O_3 structure remained almost unaltered after the reduction treatment in each case.

When Si-Beta and Al-Beta zeolites were used as supports, the metal particle size and their distribution as results of Pt and Pd incorporation onto the solid surface were slightly different depending on the type of metal. Thus, Pt incorporation onto Beta zeolites was quite homogeneous resulting in Pt nanoparticles sizes of 2–3 and 4–5 nm for Si-Beta and Al-Beta samples, respectively; while bigger metal nanoparticles (>5 nm) and less homogeneous distribution were observed with Pd incorporation on Beta zeolites when comparing with alumina samples (Tables 1 and 2). Besides, the presence of Pt and Pd metallic species on samples was also evidenced by the X-rays patterns of zeolites in Fig. 1 [22]. In all the cases, the X-rays patterns also showed the characteristic peaks of BEA-type structure with relatively high crystallinity (>85–90%), while any impurity phases were detected [17]. Thus, the diffractograms obtained for these Me-zeolites revealed that the zeolitic structure remained almost unaltered after both metal impregnation and posterior thermal treatments.

In the case of Pt-MCM-41 supported materials, the presence of Pt (average size by TEM between 2 and 4 nm) metal particles could also be observed in the X-rays diffractograms of Pt/Si-MCM-41 and Pt/Al-MCM-41 samples (Fig. 2), this confirming the TEM measurements observations (Table 3). These small Pt nanoparticles were present in mesoporous samples with Pt contents ranging from 1.8 to ≈4.0 wt%.

In the case of Pd/MCM-41 samples, Pd metal particles with average size of 11–13 nm and 7–8 nm were observed by TEM measurements for Pd/Si-MCM-41 and Pd/Al-MCM-41 samples, respectively (Table 3). These observations were also confirmed by the X-rays diffractograms of both Pd/Si-MCM-41 and Pd/Al-MCM-41 samples shown in Fig. 2. Nevertheless, the conjoint existence of Pd^0 and PdO species was detected in both Pd-based mesoporous materials [22].

With respect to the MCM-41 structure, the signals observed in the region of 0–5° of 2θ in the XRD spectra of Pt/ and Pd/MCM-41

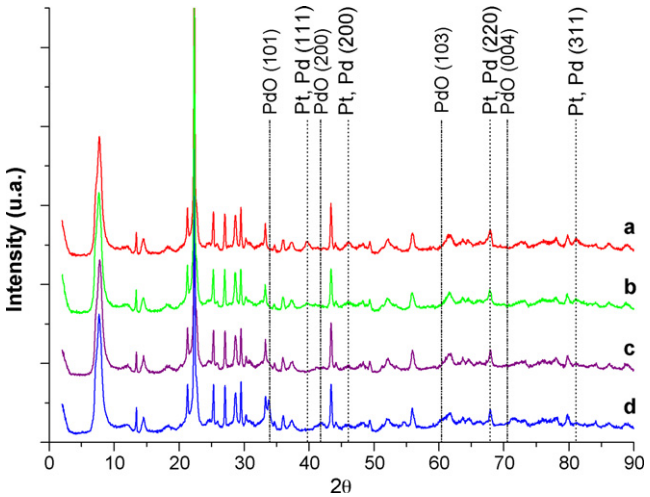

Fig. 1. X-rays patterns of calcined Me-zeolites: (a) 0.8 wt%Pt/Si-Beta, (b) 0.9 wt%Pt/Al-Beta, (c) 0.8 wt%Pd/Si-Beta, and (d) 1.2 wt%Pd/Al-Beta.

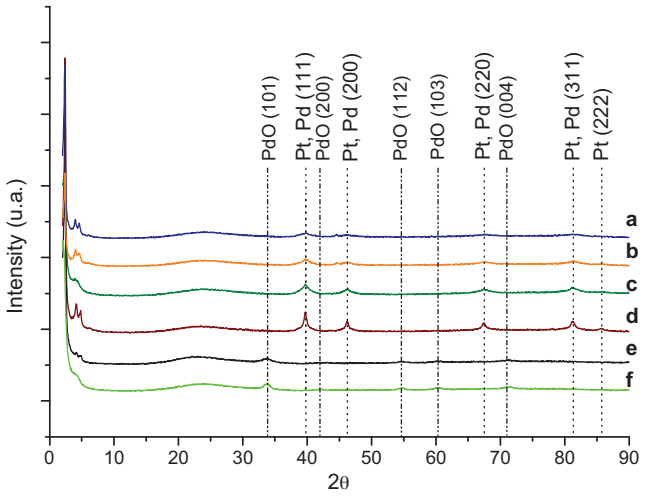

Fig. 2. X-rays patterns of calcined Me-MCM-41 materials: (a) 1.9 wt%Pt/Si-MCM-41, (b) 1.8 wt%Pt/Al-MCM-41, (c) 3.9 wt%Pt/Si-MCM-41, (d) 4.1 wt%Pt/Al-MCM-41, (e) 1.4 wt%Pd/Si-MCM-41, and (f) 1.4 wt%Pd/Al-MCM-41.

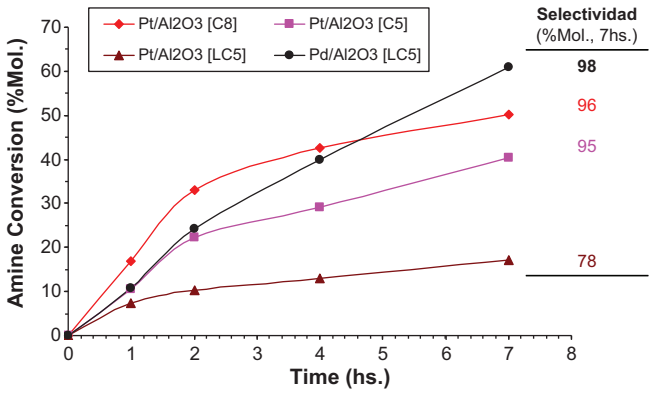

Fig. 3. Catalytic activity of Pt/ and Pd/Al_2O_3 synthesized catalysts in the reductive amination of ketones with piperidine (at 100 °C and P_{H_2} = 5 bars during 7 h).

samples are indicative of structures analogous to M41S type materials [23]. In general (see Fig. SI-7 in supplementary information), both Si-MCM-41 and Al-MCM-41 mesoporous materials present X-ray patterns characterized by: (i) an intense and broad peak at very low diffraction angle which indicates a hexagonal-type structure with long distance order, and (ii) week signals between 3° and 5° of 2θ diffraction angles which could be less or more defined peaks depending on the relatively lower or higher regularity of the hexagonal tubular structure. In this sense, it can be concluded from data of Fig. 2 that there were no significant differences at the low diffraction angle region of the spectra between the X-rays patterns obtained after metal incorporation on MCM-41-type supports and the corresponding pure Si-MCM-41 and Al-MCM-41 samples (see Fig. SI-7 in supplementary information). Nevertheless, some slight shift of the low diffraction angle peak to higher angle of 2θ were observed for Al-MCM-41 samples containing 1.8 wt% and 4.1 wt% of Pt, as well as for 1.4 wt%Pd/Si-MCM-41 material (see Fig. 2b, d and e, respectively, and also Fig. SI-8 in supplementary information), while this shift was negligible for the second group of signals in the 3–5° of 2θ diffraction angle region. As it was already reported [24], this shift could be assigned to some minimal contraction in the MCM-41 structure occurring for example after thermal treatments of pure siliceous and Al-containing MCM-41 materials, this fact producing as a consequence some slight decrease on surface area and/or pore volume. In addition, a decrease of the second group of signals (between 3° and 5° of 2θ diffraction angle) can be observed for both Pd/Si-MCM-41 and Pd/Al-MCM-41 samples (see Fig. 2e and f, and also Fig. SI-8 in supplementary information). This intensity decrease of signals could be associated to a relative lost of regularity of hexagonal channels, this effect being non detrimental for MCM-41 structure itself [24]. Summarising, it is reasonable to conclude from XRD patterns that MCM-41 structures remained practically unaltered after Pt and Pd incorporations on solids.

On the other hand, and as it can be seen from data of Table 3, the decrease in surface areas observed with respect to the conventional Si-MCM-41 and Al-MCM-41 supports were as expected taking into account the corresponding amount of metal incorporated on solid in each case. Besides, the decrease in the pore volume values measured was also reasonable and comparable for practically all the Me-mesoporous samples, even with samples containing high metal contents (i.e. ≈4.0 wt% Pt loadings). The only appreciable decrease in pore volume took place with Pd/Si-MCM-41 sample mainly due to the bigger size of Pd nanoparticles (11–13 nm) in this case. In light of these results, it is quite reasonable to conclude that metal nano-particles do not produce pore blocking of mesoporous samples, this effect being negligible in the case of Pt containing samples and minimized in the case of Pd-based materials.

3.2. Catalytic activity of Pt/ and Pd/γ-Al_2O_3 materials

In our previous work [10], we have well established the optimal reaction conditions to apply for model reductive amination studies. Thus, standard evaluation of both commercial and home-made Pd, and Pt-based catalysts was performed by mixing equimolecular amounts (6 mmol) of piperidine as secondary amine and cyclohexanone as carbonyl compound together with the catalyst in the absence of solvent. Under these conditions, good and similar levels of catalytic activities (TON ≈ 300–380, calculated as moles of products/moles of metal on catalyst) could be achieved for both Pd-, and Pt-based commercial samples [10].

In order to study the influence of alumina pre-treatments in the catalytic activity of Pt/ and Pd/Al_2O_3 supported catalysts, the alumina support was submitted before metal incorporation to two different treatments: (i) calcination at 500 °C [C5] or 800 °C [C8], and (ii) lyophilisation [L] + calcination at 500 °C [LC5]. Thus, samples named as Pt/ and Pd/Al_2O_3 [C5], Pt/ and Pd/Al_2O_3 [C8], and Pt/ and Pd/Al_2O_3 [LC5] were obtained, respectively (see Section 2). All Pt/ and Pd/Al_2O_3 samples were calcined at 400 °C and then reduced at 350 °C before their catalytic evaluation in the reductive amination of cyclohexanone with piperidine (model reaction), the results being shown in Fig. 3.

In general, the catalytic results of Fig. 3 revealed that Pt/Al_2O_3 calcined samples were much more active than Pt/Al_2O_3 lyophilised ones. Thus, Pt/Al_2O_3 [C5] and Pt/Al_2O_3 [C8] materials presented moderate to high amine conversions (Fig. 3), with TON of 1033 and 790 at 7 h of reaction, respectively. At the same time, selectivities to the tertiary amine upper than 95% were attained at 7 h of reaction in both cases (Fig. 3). In case of Pt/Al_2O_3 [LC5] lyophilised sample, amine conversions at 7 h of reaction inferior to 20% (TON = 448) were achieved, this demonstrating that lyophilisation pre-treatment of alumina before metal deposition produces Pt-catalysts with low activity for the reductive amination reaction. It is reasonable to conclude that the type of alumina support pre-treatment has a great impact on the final catalytic activity of Pt/γ-Al_2O_3 materials. While lyophilisation produced high surface area γ-Al_2O_3 with high content of hydroxyl groups onto the solid surface, calcination treatment decreased the amount of these exposed hydroxyl species giving a less acidic support surface. Thus, an adequate calcination process at 500 °C (or even superior) guarantied the preparation of efficient Pt/Al_2O_3 catalysts for the selective reductive amination of ketones. The results afore-

mentioned for Pt/Al_2O_3 [C5] (TON = 1033) were higher than those reached with Pt/Al_2O_3 commercial catalysts already commented [10].

On the contrary to the low catalytic activities observed with Pt/Al_2O_3 lyophilised samples, when this lyophilised alumina was used as support for preparation of a Pd supported material (Pd/Al_2O_3 [LC5]); a marked enhancement of both amine conversion (61%, Fig. 5) and catalytic activity (TON = 924) was observed in comparison with results obtained with the only calcined Pd-based sample (Pd/Al_2O_3 [C5]). This fact demonstrates once again that physical and chemical properties of oxides used as supports have an enormous influence on the final catalytic activity of Me-catalysts, but also that support properties modifications could be beneficial or detrimental to the catalytic activity found depending on the type of metal to be incorporated.

3.3. Catalytic activity of Pt/ and Pd/Beta zeolites

Pt and Pd based catalysts supported on Si-Beta and Al-Beta zeolites were tested in the reductive amination of cyclohexanone with piperidine. As can be seen in Table 4, the Pt/Al-Beta catalyst showed the best catalytic activity (TON = 1610, conversion = 37% and selectivity = 96%) in comparison with the Pt/Si-Beta analogous sample, and even better than those observed with the Pd/Beta catalysts. The yields to the desired product achieved with Pt/Al-Beta catalyst were comparable to those attained with Pt commercial catalysts tested in this work, these being excellent results for a Pt-catalyst in reductive amination reactions. From these data it is possible to infer that the presence of strong acid sites (observed by pyridine adsorption–desorption IR spectroscopic measurements, see supporting information) is essential for the Pt/Al-Beta catalytic activity. This acidity could favour: (i) the C=O group activation by selective adsorption on the acid center, and (ii) the major Pt-support interaction due to the electropositive effect of the Al with respect to the Si [25], which is able to increase metal reducibility. Nevertheless, the possibility to Pt–Al alloys formation in this type of samples could not be ruled out.

Taking into account that both Pt and Al contents in Pt/Al-Beta catalyst could play an important role in the catalytic activity observed during the reductive amination process, we studied the effect of Pt loading variation, as well as the influence of the Si/Al molar ratio changes in Pt/Al-Beta samples. As can be seen in Fig. 4A, a strongly decrease in the catalytic activity (from 1610 to <400 in TON) of the Pt/Al-Beta (Si/Al = 50) samples occurs when the amount of Pt in the solid was increased from 0.9 to 3.4 wt%. This trend is also coincident with an increase in the Pt particle size diameter at higher metal loading, as well as a decreasing in metallic dispersion values (data not shown). These observations lead us to conclude that by increasing the Pt content in Pt/Al-Beta samples, the synergic effect of Pt and Al presence is loosed probably due to (i) the less effective interaction between the bigger Pt particles and the Al in the zeolitic framework, and (ii) the lower amounts of Pt surface effective for H_2 dissociation, even when the total amount of Pt in the solid sample is higher.

In the case of the influence of Si/Al molar ratio change in Pt/Al-Beta, a marked enhancement in catalytic activity was encountered with the increase of Al content in zeolites (Fig. 4B). In this sense, catalytic activity grew from 1610 to 1870 (expressed in TON) when Si/Al molar ratio changed from 50 to 25. Of course, the later TON values were clearly superior to that obtained with Pt/Si-Beta (Si/Al = ∞) sample without Al in the zeolitic framework (Fig. 4B). These results confirm our previous hypothesis that the presence of acid sites in Pt/Al-Beta samples favours both H_2 dissociation on Pt and carbonyl compounds activation for reductive amination process.

In the case of Pd, the above-mentioned Al effect was also observed, although in a minor extent. Thus, Pd/Si-Beta sample was non active for this process, while Pd/Al-Beta material showed low catalytic activity. Probably, the Pd incorporation onto this type of materials requires a different treatment, and following this idea, we are now developing new Pd supported on Beta materials using different metal deposition processes others than conventional impregnations.

Summarising, Pt/Al-Beta catalyst showed the best catalytic activity in the reductive amination of ketone with tert-amine yields comparable to those attained with Pt commercial samples, these results being interesting and very promising for the use of these Pt-based catalysts in cascade type reaction in liquid phase involving some reductive amination reaction step.

3.4. Catalytic activity of Pt/ and Pd/MCM-41 mesoporous materials

The most relevant results of the reductive amination catalytic experiments performed with Pt/ and Pd/MCM-41 mesoporous materials are summarized in Table 5. In this case, Pd/Al-MCM-41 catalyst presented the best levels of amine conversion (>40%) and selectivity to the desired tert-amine (>95%). TON values attained with Pd-containing MCM-41 catalysts were upper than 500, these values being at least comparable to those achieved with the same support material but with Pt as hydrogenating function. Nevertheless, both 1.9 wt%Pt/MCM-41 and 1.8 wt% Pt/Al-MCM-41 samples offered lower amine conversions when comparing with Pd-based materials, while selectivities to the tert-amine obtained were around 90%. This tendency is contrary to that observed with Me/Beta catalysts, in which Pt-containing materials showed better catalytic performances than their Pd analogues. Moreover, catalytic behaviour comparison between 1.7 wt%Pt/Al-Beta with TON = 1038 (Fig. 4) and 1.8 wt%Pt/Al-MCM-41 with TON = 729 showed that Al-Beta is quite superior as specific acid support for this reaction. Taking this into consideration, it is possible to conclude that the type of support enormously influences the catalytic activity when comparing MCM-41 mesoporous materials with Beta zeolites in the reductive amination. If we consider that, in general, (i) any limitation to both reactants and products diffusion occurs during reaction inside the zeolitic pores that could inhibit or reduce the catalytic activity of Me-Beta samples, and (ii) a negligible or minimum pore blocking occurs inside the channels of MCM-41 materials with metal nanoparticles incorporation (slight decrease in pore volumes and surface areas were observed in most of the samples); the observed differences indicate that a major (or better) interaction between the support and the impregnated metal takes place in Al-Beta zeolites. These interactions mainly depend on the type of metal involved (metal reducibility, particle size), and the acid strength of the support.

3.5. Comparison of Pt and Pd catalysts prepared in this study with commercial samples

The catalytic activity calculated by metal center (TON) of the best Pt- and Pd-based materials prepared in this study is compared with the corresponding metallic commercial catalysts in Fig. 5. In all the cases, the selectivities to tert-amine obtained were superior to 95%. For Pt-containing catalysts, the 1.9 wt%Pt/Al_2O_3 [C8] material presented similar catalytic activity than the Pt/Al_2O_3 commercial sample, while the 0.9 wt%Pt/Al-Beta (Si/Al = 50) zeolite surpassed in $\approx$1.5–1.6 times the TON values achieved with both Pt/C and Pt/Al_2O_3. Moreover, when 0.9 wt%Pt/Al-Beta (Si/Al = 25) optimized catalyst was used the catalytic activity achieved (TON = 1870) was practically twice when compared with both Pt-containing com-

Table 4
Catalytic activity of Pt/and Pd/Beta materials in the reductive amination of cyclohexanone with piperidine.[a]

Catalyst (metal content, wt%)	Amine conversion (mol%)	Selectivity to tert-amine (mol%)	TON (mol/mol Me)
(0.9) Pt/Al-Beta	37	96	1610
(0.8) Pt/Si-Beta	22	51	1075
(1.2) Pd/Al-Beta	12	58	212
(0.8) Pd/Si-Beta	0	0	0

[a] With 0.03 g of catalyst, at 100 °C, and P_{H_2} = 5 bars during 7 h (conversion based on piperidine).

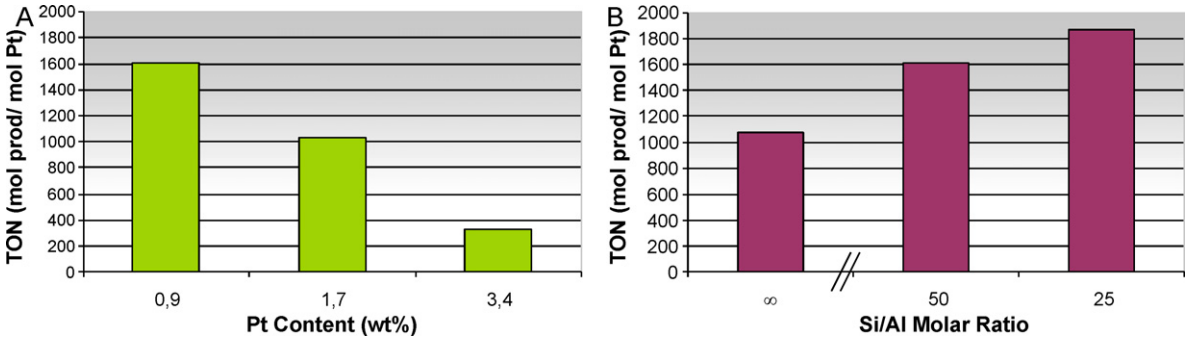

Fig. 4. Influences of Pt (A) and Si/Al molar ratio (B) on the catalytic activity (TON) of Pt/Al-Beta catalysts in the reductive amination of cyclohexanone with piperidine (at 100 °C and P_{H_2} = 5 bars during 7 h).

Table 5
Catalytic activity of Pt/ and Pd/MCM-41 mesoporous materials in the reductive amination of cyclohexanone with piperidine.[a]

Catalyst (metal content, wt%)	Amine conversion (mol%)	Selectivity to tert-amine (mol%)	TON (mol/mol Me)
(3.9) Pt/Si-MCM-41	40	95	400
(4.1) Pt/Al-MCM-41	39	98	390
(1.9) Pt/Si-MCM-41	33	87	683
(1.8) Pt/Al-MCM-41	34	91	729
(1.4) Pd/Si-MCM-41	49	96	742
(1.4) Pd/Al-MCM-41	33	95	500

[a] With 0.03 g of catalyst, at 100 °C, and P_{H_2} = 5 bars during 7 h (conversion based on piperidine).

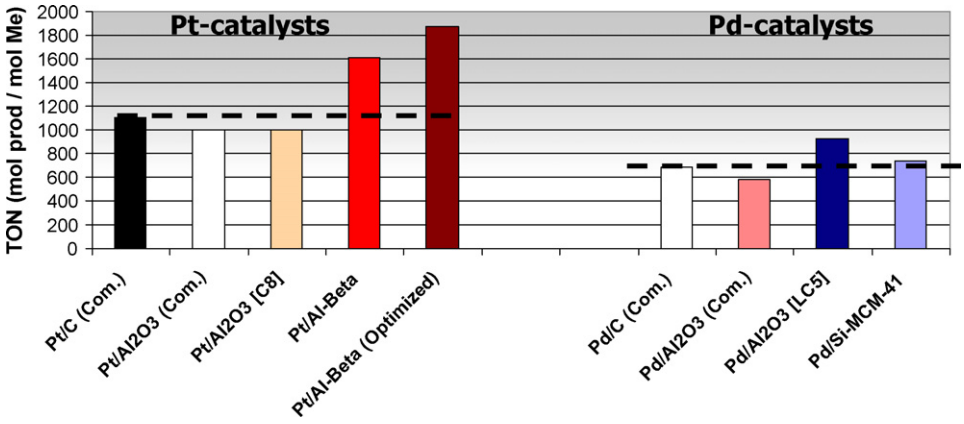

Fig. 5. Catalytic activity (TON) of Pt and Pd catalysts in the reductive amination of cyclohexanone with piperidine (0.003 mmol of Pt or 0.005 mmol of Pd, at 100 °C and P_{H_2} = 5 bars during 7 h).

mercial catalysts. This fact demonstrates the excellent and very promising performance of the Pt/Al-Beta catalyst in the selective reductive amination of ketones.

In general, Pd-based catalysts possessed minor catalytic activities than that observed with Pt-containing samples. Nevertheless, it is clearly observed that either the Pd/Al_2O_3 [LC5] sample or the 1.4 wt%Pd/Si-MCM-41 mesoporous material presented catalytic activities (TON) higher than the attained with Pd/C and Pd/Al_2O_3 commercial samples. The results obtained with the 1.4 wt%Pd/Al_2O_3 [LC5] catalyst also evidenced that the process of alumina lyophilisation (previous to the Pd nano-particles deposition) improved the catalyst efficiency in the reductive amination under mild reaction conditions.

4. Conclusions

Catalysts possessing more than one catalytic function (redox and Brönsted and/or Lewis acid sites) based on Pt and Pd nanoparticles supported on solid matrix with well controlled structure and porosity, such as Beta zeolite, MCM-41 mesoporous material, and also regular alumina, have been developed. Some of these catalysts demonstrated their high efficiency in the selec-

tive reductive amination of ketones in liquid phase and in absence of solvent by working under mild reaction conditions. Thus, the Pt/Al-Beta showed the best catalytic activity (amine conversion of 37%, TON = 1610) with a selectivity to the desired tert-amine >95% when cyclohexanone was used as reactant. In addition, optimization of the Pt loading, and mainly the Al content in Pt/Al-Beta sample let to enhancement in the catalytic activity (TON = 1870), while selectivity to the tert-amine remained unaltered. When Pt/Si-MCM-41 and Pt/Al-MCM-41 materials were used, lower catalytic activities by metal center (TON) were attained, the results being slightly improved when metallic Pd was used instead of Pt. In such way, Pd/Si-MCM-41 and Pd/Al-MCM-41 catalysts showed catalytic activities superior to those obtained with commercial catalysts, such as Pd/C and Pd/Al_2O_3. In the case of γ-Al_2O_3 based materials, our study demonstrates that the conditions of support pre-treatment and/or calcination previous to metal deposition, as well as the ulterior thermal treatments or activation to which the solids are exposed before the catalytic evaluation, have enormous influence on the final catalytic activity observed.

Acknowledgements

Financial support by Ministerio de Ciencia e Innovación (MICINN) of Spain (CTQ-2008-06446), CSIC (PIE-200980I063), and COST Action CM0903 (UBIOCHEM) is gratefully acknowledged. Authors also thank M. Arribas for help in adsorption measurements.

Appendix A. Supplementary data

Supplementary data associated with this article can be found, in the online version, at doi:10.1016/j.cattod.2011.05.013.

References

[1] J.J. Birtill, J. Mol. Catal. A: Chem. 305 (2009) 183.
[2] Y.S. Higassio, T. Shoji, Appl. Catal. A: Gen. 221 (2001) 197.
[3] N.R. Candeias, C.A.M. Afonso, J. Mol. Catal. A: Chem. 242 (2005) 195.
[4] S. Shimizu, T. Niwa, T. Shoji, JP 02011577 (1988). Koei Chemical Co. Ltd.
[5] V.R. Rani, N. Srinivas, S.J. Kulkarni, K.V. Raghavan, J. Mol. Catal. A: Chem. 187 (2002) 237.
[6] K.G. Liu, A.J. Robichaud, Tetrahedron Lett. 46 (2005) 7291.
[7] P. Vairaprakash, M. Periasamy, J. Org. Chem. 71 (2006) 3636.
[8] A. Baiker, J. Kijenski, Catal. Rev. Sci. Eng. 27 (1985) 653.
[9] A. Corma, T. Ródenas, M.J. Sabater, Chem. Eur. J. 16 (2010) 254.
[10] M.E. Domine, M.C. Hernández-Soto, Y. Pérez, Catal. Today 159 (2011) 2.
[11] T. Mallat, A. Baiker, in: R.A. Sheldon, H. van Bekkum (Eds.), Fine Chemical through Hetereogeneous Catalysis, Wiley-VCH, Weinheim, 2001, p. 247.
[12] M. Haniti, S.A. Hamid, J.M.J. Williams, Chem. Commun. (2007) 725.
[13] K. Fujita, Z. Li, N. Ozeki, R. Yamaguchi, Tetrahedron Lett. 44 (2003) 2687.
[14] D. Gnanamgari, E.L.O. Sauer, N.D. Schley, C. Butler, C.D. Incarvito, R.H. Crabtree, Organometallics 28 (2009) 321.
[15] P. Dolezal, O. Machalicky, M. Pavelek, P. Kubec, K. Hradkova, R. Hrdina, R. Sulakova, Appl. Catal. A: Gen. 286 (2005) 202.
[16] D.M. Roundhill, Chem. Rev. 92 (1992) 1.
[17] A. Corma, M.E. Domine, S. Valencia, J. Catal. 215 (2003) 294.
[18] A. Corma, V. Fornés, M.T. Navarro, J. Pérez-Pariente, J. Catal. 148 (1994) 569.
[19] T.F. Baumann, A.E. Gash, S.C. Chinn, A.M. Sawvel, R.S. Maxwell, J.H. Satcher, Chem. Mater. 17 (2005) 395.
[20] A. Mastalir, B. Rác, Z. Király, A. Molnár, J. Molec. Catal. A Chem. 264 (2007) 170.
[21] A. Cabiac, T. Cacciaguerra, P. Trens, R. Durand, G. Delahay, A. Medevielle, D. Plée, B. Coq, Appl. Catal. A: Gen. 340 (2008) 229.
[22] A. Morlang, U. Neuhausen, K.V. Klementiev, F.-W. Schütze, G. Miehe, H. Fuess, E.S. Lox, Appl. Catal. A: Gen. 60 (2005) 191.
[23] J.S. Beck, C. Chu, Y. Johnson, C.T. Kresge, M.E. Leonowicz, W.J. Roth, J.C. Vartuli, WO Pat 11390, 1991.
[24] B. Marler, U. Oberhagemann, S. Votrmann, H. Gies, Micropor. Mater. 6 (1996) 375.
[25] P.L. Arias, J.F. Cambra, B. Güemes, V.L. Barrio, R. Navarro, B. Pawelec, J.L.G. Fierro, Fuel Proc. Tech. 64 (2000) 117.